Journal of the European Ceramic Society **10** (1992) 41–50

The Effect of Yttria Additions on the Composition of O′-Sialons Prepared by Pressureless Sintering

J. Sjöberg,[a] C. O'Meara[b]

[a] Department of Inorganic Chemistry and [b] Department of Physics, Chalmers University of Technology and University of Göteborg, S-412 96 Göteborg, Sweden

&

R. Pompe

Swedish Ceramic Institute, Box 5403, S-402 29 Göteborg, Sweden

(Received 27 September 1991; accepted 8 November 1991)

Abstract

The compositional range of O′-sialons, $Si_{2-x}Al_xN_{2-x}O_{1+x}$, has been investigated for different preparative conditions. Samples made by pressureless sintering with and without additions of yttria, covering a compositional range corresponding to $0{\cdot}04 < x < 0{\cdot}60$ in the O′-sialon formula were compared. The compositions were analysed by monitoring the change in unit cell dimensions along the compositional range, by calculating interatomic bond distances and site occupancies in the O′-sialon using Rietveld refinements and by EDX analysis. The possible inclusion of yttrium atoms in the O′-sialon structure was investigated by EDX analysis and X-ray diffraction and the preferred growth directions of the crystals were determined. A maximum of ≈ 10% of the silicon atoms were found to be replaced by aluminium in the yttrium-free samples and > 20% in samples prepared with additions of yttria as a sintering aid. The amount of yttrium in O′-sialon crystals was found to be very low, < 1·5 wt%.

Der Zusammensetzungsbereich von O′-Sialon-Keramiken, $Si_{2-x}Al_xN_{2-x}O_{1+x}$, wurde für verschiedene Herstellungsbedingungen untersucht. Es wurden Proben miteinander verglichen, die mittels drucklosen Sinterns, mit und ohne Zugabe von Yttriumoxid, hergestellt wurden, wobei ein Zusammensetzungsbereich entsprechend der O′-Sialon-Formel von $0{\cdot}04 < x < 0{\cdot}60$ betrachtet wurde. Die Zusammensetzungen wurden bestimmt, indem die Änderung der Abmessungen der Einheitszelle entlang des Zusammensetzungsbereiches verfolgt wurde. Dies geschah mittels Berechnung der interatomaren Bindungsabstände und der Gitterplatzbelegung in O′-Sialon, wobei Rietveld-Verfeinerung und EDX-Analysen herangezogen wurden. Der mögliche Einbau von Yttrium-Atomen in der O′-Sialon-Struktur wurde mit Hilfe von EDX-Analysen und Röntgenbeugung untersucht. Des weiteren wurden die bevorzugten Wachstumsrichtungen der Kristalle bestimmt. In Yttrium-freien Proben werden Silizium-Atome bis zu höchstens 10% durch Aluminium substituiert. Bei der Zugabe von Yttriumoxid als Sinterhilfe können mehr als 20% ersetzt werden. Der Gehalt an Yttrium in den O′-Sialon-Kristallen ist sehr gering (< 1·5 Gew.%).

Un domaine de composition d'O′-sialons, $Si_{2-x}Al_xN_{2-x}O_{1+x}$, été étudié pour différentes conditions de préparation. Des échantillons frittés sous pression normale avec et sans addition d'yttrine dans un domaine de composition correspondant à $0{\cdot}04 < x < 0{\cdot}60$ dans la formule des O′-sialons ont été comparés. Les compositions ont été analysées en contrôlant le changement de dimension des paramètres du réseau, en calculant les distances interatomiques de liaison et l'occupation des sites dans l'O′-sialon par raffinage Rietveld et par EDX. La possible intrusion d'atomes d'yttrium dans la structure O′-sialon a été étudiée par EDX et diffraction de rayon X, et les directions préférentielles de croissance des cristaux ont été déterminées. Un maximum d'environ 10% d'atomes de silicium remplacés par de

Journal of the European Ceramic Society 0955-2219/92/$5.00

l'aluminium a été trouvé dans les échantillons ne contenant pas d'yttrium et plus de 20% dans les échantillons contenant de l'yttrium comme agent de frittage. La quantité d'yttrium trouvé dans les cristaux d'O'-sialon est trés faible (< 1·5 wt%).

1 Introduction

In the phase system Si_3N_4–SiO_2–Al_2O_3–AlN several regions of solid solubility have been established, e.g. the β'-sialon, the O'-sialon and the sialon polytypoids.[1] The existence of phases with varying stoichiometry is important in the design of phase compositions in many sialon materials. While the phase region for the β'-sialons, $Si_{6-z}Al_zN_{8-z}O_z$, with $0 < z < 4{\cdot}2$, has been systematically studied with respect to temperature and pressure,[2-6] the situation for the O'-sialons, $Si_{2-x}Al_xN_{2-x}O_{1+x}$, is less clear. The data now available from different investigations show a considerable scatter[4,7-15] and it is likely that differences in preparation conditions are responsible for the large variations observed.

The preparation of sialon materials generally requires the presence of a transient liquid, from which the sialon grains precipitate.[12] It is common to add sintering aids, e.g. Y_2O_3 or MgO, to the powder mixture used, in order to reduce the melting temperature and to lower the viscosity of the melt. The use of a lower temperature also reduces the risk of thermal decomposition of the phases which are formed.[13] Although large cations from the sintering additives are not usually found in the structure of the sialon system present in the Si_3N_4–SiO_2–Al_2O_3–AlN system, the various conditions of preparation may influence the achievable compositional ranges. This would probably be more important in the case of O'-sialons than for β'-sialons, where the sintering aids are likely to promote the formation of α'-sialon, thereby leaving the β'-sialon region and moving out of the sialon-phase region.[16-20] The α'-sialon, which is isostructural with α-Si_3N_4, accommodates for its stabilisation additional cations, such as yttrium and calcium, in the large interstitial sites present in the structure. In the structures of β'-sialon and O'-sialon, there are also sites which are large enough to accomodate large cations, but these sites seem to be less favourable than those in α'-sialon. Therefore, also for the formation of O'-sialon, the use of sintering aids in the preparation is mainly reflected in the formation of secondary phases.[13,14,21]

This work is concerned with the influence of Y_2O_3 on the possible compositional variations of O'-sialons. For a comprehensive assessment, a combination of experimental techniques was used: lattice parameters were determined from X-ray diffraction data; crystallographic information was derived from X-ray, neutron and electron diffraction data; and compositional analysis was carried out by EDX analysis in TEM/STEM.

2 Experimental

2.1 The samples

Two main sets of samples were used in this study, one—set A—with compositions in the phase plane Si_3N_4–SiO_2–Al_2O_3–AlN, and another—set B—also containing yttrium. The samples were prepared by mixing α-Si_3N_4, SiO_2 xerogel, Al_2O_3 and, in the case of set B, Y_2O_3. Five samples, 1, 2, 3, 4 and 5, were prepared for set A with different proportions of the starting powders in order to achieve compositions corresponding to $x = 0{\cdot}04$, 0·10, 0·16, 0·24 and 0·40, respectively, in the above general formula of O'-sialons. For set B, seven samples, 6, 7, 8, 9, 10, 11 and 12, with compositions corresponding to $x = 0{\cdot}06$, 0·12, 0·16, 0·20, 0·30, 0·40 and 0·60, respectively, were prepared. The Y_2O_3 added accounted for 5 wt% of the sample and the proportion of SiO_2 in the powder mixture was increased for the compositions of these samples to become equivalent to $Si_{2-x}Al_xN_{2-x}O_{1+x} + Y_2Si_2O_7$. The powders of both sets were mixed/milled in an agate ball mill with ethanol and pressing agents. The dried powder mixtures were then formed, cold isostatically pressed at 275 MPa and the remaining ethanol and pressing agents were driven off at 573 K prior to sintering. The silica introduced by milling (typically 2·5% of the total powder weight) was included in the compositional balance of the samples. The samples of set A were sintered at 2093 K for 30 minutes in a nitrogen atmosphere under a protective powder of preoxidised Si_3N_4 in a graphite resistance furnace. For set B, two different sintering conditions were used to explore the effect of temperature. Samples 6, 8, 11 and 12 were sintered at 1928 K for 2 h while sintering at 1973 K for 30 min followed by a dwell at 1923 K for 2 h was applied to samples 7, 9, 10 and 11. The sinterings of samples of set B were carried out in a platinum-wound alumina tube furnace. The samples of set B are henceforth denoted 6L, 8L, 11L, 12L, 7H, 9H, 10H and 11H to indicate whether a high or low sintering temperature was used.

In addition to these samples, a sample 13 was prepared from an amorphous powder with a composition equivalent to that of Si_2N_2O with additions of Al_2O_3 and Y_2O_3 (6 and 10 wt%,

respectively). The preparation of the amorphous powder is described elsewhere.[22] No further increase of the amount of silica was made, except for the amount of silica eroded during milling from the agate ball mill. This sample was sintered at 1928 K for 1 h in a graphite resistance furnace. The most important data on the preparation of the powder samples are summarised in Table 1.

2.2 Determination of phase compositions and lattice parameters

The positions of the diffraction peaks were determined by the Hägg–Guinier film technique, using a 114 mm diameter Huber focusing camera with $CuK_{\alpha 1}$ radiation from a sealed X-ray tube which was monochromatised in a bent quartz crystal. A small amount of $Pb(NO_3)_2$ was added as an internal standard. The films were scanned by an optical line scanner using the evaluation programs Scan3 and Scanpi7.[23] The phase compositions were determined by comparing the data obtained with data from the JCPDS database. Distinction between α- and β-Si_3N_4, on the one hand, and α'- and β'-sialons, on the other, was made from careful determinations of lattice parameters which were compared to the unit cell dimensions determined for a commercial α-Si_3N_4 powder and β-Si_3N_4 prepared by nitridation of Si in N_2. Data from a 2θ diffractometer were used as a complement to the film data to detect minor amounts of secondary phases. Here, nickel-filtered CuK_α radiation was used. Lattice parameters were refined with the least squares program Pirum.[24] For consistency in the calculations of the unit cell dimensions of O'-sialon, the same reflections were used for all samples.

2.3 Microstructure and composition

The microstructures of samples 11L and 13 were examined in a Jeol 2000FX TEM/STEM instrument equipped with a Link Systems AN 10000 EDX spectrometer. Thin foils of the samples were prepared from 3-mm cylinders cut from the sintered bodies using a Gatan ultrasonic disc cutter. The cylinders were then sliced into 1-mm thick discs and ground to approximately 150 μm in a Minimet precision grinder. The discs were dimple ground on one side to an approximate thickness of 20 μm and ion-beam milled to perforation from both sides at an angle of 15°. The samples were then coated with a thin film of carbon. Selected area electron diffraction (SAED) was used for the identification of crystalline phases. The results of SAED were coupled to both elemental analysis as determined by EDX and the results of X-ray diffractometry. For sample 11L EDX analysis was carried out on 10 O'-sialon crystals carefully selected in order to minimise the possibility of additional cation contribution to the analysis from the glassy phase in the microstructure. The compositional analysis of the O'-sialon crystals in sample 13 is described in an earlier work.[25]

2.4 Neutron and X-ray diffraction data for Rietveld analysis

Samples 2, 3, 4, 10H and 11H were crushed to powder and leached in hot sodium hydroxide (1 M) and hot aqua regia to remove any remaining glassy

Table 1. Preparative conditions

Sample	*Intended x-value*	*Starting powders*	*Sintering temperature (K)*	*Sintering time (h)*
1	0·04			
2	0·10			
3	0·16			
4	0·24			
5	0·40	SN, SO, AlO	2093	0·5
6L	0·06			
8L	0·16			
11L	0·40			
12L	0·60		1928	2
7H	0·12			
9H	0·20			
10H	0·30			
11H	0·40	SN, SO, AlO, YO	1973/1923	0·5/2
13	0·12	*a*-SiNO, AlO, YO	1928	1

SN = α-Si_3N_4 (SN-E-10, UBE, Japan); SO = spray-dried silica sol (Bindsil 15-500, EKA Nobel AB, Sweden); AlO = Al_2O_3 (APK, Sumitomo, Japan); YO = Y_2O_3 (H.C. Starck, FRG); *a*-SiNO = amorphous silicon oxynitride.[25]

phase and metal impurities and finally washed in hot deionised water. Neutron diffraction data for these five samples were collected at the pulsed neutron source ISIS, Rutherford–Appleton Laboratory (RAL), UK, using the Polaris medium resolution diffractometer,[26] further details of which are given in a separate work.[27] For comparison, neutron diffraction data for sample 10H were also collected at the reactor source R2 at Studsvik, Sweden. Here, a 2θ powder diffractometer equipped with ten detectors separated by 1·36° was used. Data in the range 14·6° to 125·0° in 2θ in steps of 0·08°, with 180 s dwell at each step, were acquired using neutrons with a wavelength of 1·484 Å. X-ray data for Rietveld analysis were collected on a STOE powder diffractometer which receives $CuK_{\alpha 1}$ radiation from a rotating anode source. The sample was glued onto a polymeric film and vertically mounted on the diffractometer and exposed to the beam in a transmission mode. Data were collected in the range 10° to 120·62° in 2θ in steps of 0·02°.

The neutron diffraction data from the pulsed source were analysed with the programs TF12LS and TF15LS,[28] which were developed at ISIS to include expressions for the peak shape intrinsic to the source. The details of these refinements are presented elsewhere;[27] it should be noted, however, that the absence of a multiphase version of the programs prompted the use of an interactive procedure, where the contributions of the secondary phases present in the samples were carefully subtracted from the corrected raw data.

The neutron diffraction data from the R2 reactor and the X-ray data were analysed with the program LHPM 1.[29,30] For the neutron diffraction data from R2, a Gaussian peak shape was assumed, while for the X-ray data a pseudo-Voigt peak shape was used. In addition to the O′-sialon, α-Si_3N_4 and β′-sialon were included in the refinements which, in the final cycles for the X-ray data, covered the following parameters; three intensity-scale factors, six background parameters, zero point, four peak-shape parameters, seven lattice parameters (three for the O′- and two each for the α- and β′-phases), seven atomic coordinates and three isotropic temperature factors. For the neutron diffraction data the same parameters were refined except for the zero point and the β′-phase lattice parameters. There were only three peak-shape parameters in this case and, in addition, one occupancy factor was included. No preferred orientation or asymmetry parameters were used. Despite the etching procedure described, there was a marked contribution from an amorphous component in the X-ray data set, which might originate from the sample and/or from the film onto which the sample was mounted. This prevented refinement of parameters to the whole data set with analytical expression for the background, and thus, the low angle data were excluded from the fitting procedure. Residual electron densities left from the Rietveld refinements on X-ray data were calculated by Fourier difference analysis, using the program Fordup.[31]

Results

The phase compositions of all samples are summarised in Table 2. The secondary phases are listed for each sample in decreasing order of abundance. They are present in low amounts (<5%) in all

Table 2. Phases other than O′-sialon found after sintering

Sample	*Secondary phases*
1	α, β′
2	β′, α
3	β′, α
4	β′, α
5	β′, X, (α)
6L	α, β′
8L	β′, α
11L	β′, X, (α)
12L	β′, X
7H	β′, α
9H	β′, α
10H	β′, α, (X)
11H	β′, X, (α)

α = α-Si_3N_4; β′ = β′-sialon ($Si_{6-z}Al_zN_{8-z}O_z$); X = sialon X-phase (approx. $Si_3Al_{16}O_{12}N_2$).

Table 3. Lattice parameters determined by Hägg–Guinier film technique

Sample	*a* (Å)	*b* (Å)	*c* (Å)	*Volume* (Å^3)
Si_2N_2O[32]	8·8850(6)	5·4967(5)	4·8548(3)	237·10(3)
1	8·8807(13)	5·5973(10)	4·8550(6)	237·00(6)
2	8·8934(6)	5·4984(8)	4·8579(4)	237·56(4)
3	8·8997(9)	5·4988(7)	4·8588(4)	237·60(4)
4	8·9052(7)	5·4982(6)	4·8582(3)	237·86(4)
5	8·9112(16)	5·4976(6)	4·8596(4)	237·93(5)
6L	8·8694(12)	5·4975(10)	4·8542(8)	236·69(6)
8L	8·8919(6)	5·4980(5)	4·8547(3)	237·33(3)
11L	8·9083(18)	5·5007(11)	4·8566(8)	237·98(8)
12L	8·9191(16)	5·4964(12)	4·8583(9)	238·17(10)
7H	8·9013(7)	5·4958(5)	4·8573(3)	237·62(4)
9H	8·8990(5)	5·4980(3)	4·8560(3)	237·59(2)
10H	8·9137(8)	5·4965(4)	4·8565(2)	238·01(3)
11H	8·9254(5)	5·4974(3)	4·8593(3)	238·45(2)
13	8·885(1)	5·493(1)	4·852(1)	236·80(6)

Table 4. Results from Rietveld refinements

	Coordinates			*Temperature factor* ($Å^2$)		*Occupancy in x*
	x	*y*	*z*	*ITF*	*B*	
Polaris data						
Sample 2						
Si/Al	0·1769(2)	0·1504(3)	0·2810(5)	0·29(2)		0·17(6)
N/O1	0·2182(1)	0·1244(2)	0·6268(4)	0·37(1)		
O2	0·0000	0·2133(3)	0·2300	0·51(4)		
$R_p = 4·50$		$R_I = 3·84$				
Sample 3						
Si/Al	0·1771(2)	0·1506(4)	0·2808(6)	0·33(3)		0·20(6)
N/O1	0·2182(1)	0·1246(2)	0·6270(5)	0·40(1)		
O2	0·0000	0·2136(4)	0·2300	0·60(4)		
$R_p = 4·73$		$R_I = 3·89$				
Sample 4						
Si/Al	0·1775(2)	0·1496(4)	0·2809(7)	0·31(3)		0·36(6)
N/O1	0·2181(1)	0·1246(2)	0·6270(5)	0·31(2)		
O2	0·0000	0·2133(4)	0·2300	0·66(5)		
$R_p = 5·48$		$R_I = 4·17$				
Sample 10H						
Si/Al	0·1781(3)	0·1495(5)	0·2803(9)	0·21(4)		0·40(8)
N/O1	0·2183(1)	0·1243(2)	0·6276(7)	0·26(2)		
O2	0·0000	0·2134(5)	0·2300	0·66(7)		
$R_p = 8·63$		$R_I = 6·11$				
Sample 11H						
Si/Al	0·1783(3)	0·1497(6)	0·2803(9)	0·22(4)		0·56(8)
N/O1	0·2182(2)	0·1240(3)	0·6270(7)	0·32(3)		
O2	0·0000	0·2131(6)	0·2300	0·65(8)		
$R_p = 5·70$		$R_I = 6·97$				
R2 data						
Sample 10H						
Si/Al	0·1775(6)	0·1495(13)	0·2828(16)		−0·05(14)	0·30(8)
N/O1	0·2181(2)	0·1245(6)	0·6292(13)		0·05(7)	
O2	0·0000	0·2131(10)	0·2300		0·33(18)	
$R_p = 6·61$		$R_B = 2·76$				
XRD data						
Sample 10H						
Si/Al	0·1755(2)	0·1545(4)	0·2790(21)		0·22(7)	
N/O1	0·2149(7)	0·1175(15)	0·6275(26)		0·58(19)	
O2	0·0000	0·2114(13)	0·2300		1·58(25)	
$R_p = 4·52$		$R_B = 1·85$				

$R_p = \Sigma(Y_i^{obs} - Y_i^{calc})/\Sigma Y_i^{obs}$.
$R_I = \Sigma(I_k^{obs} - I_k^{calc})^2/\Sigma I_k^{obs}$.
$R_B = \Sigma|I_k^{obs} - I_k^{calc}|/\Sigma I_k^{obs}$.

samples except samples 1, 6L and 12L, which are at either ends of the compositional span in this investigation. In addition, in all yttrium-containing samples, considerable amounts of glassy phase were found. The lattice parameters for the O'-sialon component of all samples are given in Table 3. The lattice parameters determined from the material used in the single-crystal structure refinement is also included.[32] The only major variations between the samples are observed for the unit cell edge *a*, which is plotted as a function of the intended composition for each sample in Fig. 1.

The crystal data extracted by Rietveld refinements based on the neutron and X-ray diffraction data are given in Table 4. As reported earlier,[27] only the bond length (Si, Al)–O2 is significantly affected by the change in composition, while all bonds in the planes perpendicular to the *a*-direction of the unit cell remain unchanged within the statistical error. The bond lengths are given in Fig. 2 as a function of the

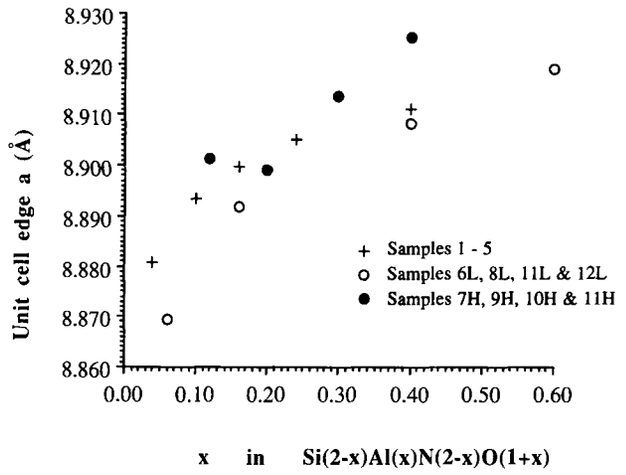

Fig. 1. Lattice parameter *a* versus composition (in *x*) as calculated from the powder mixtures.

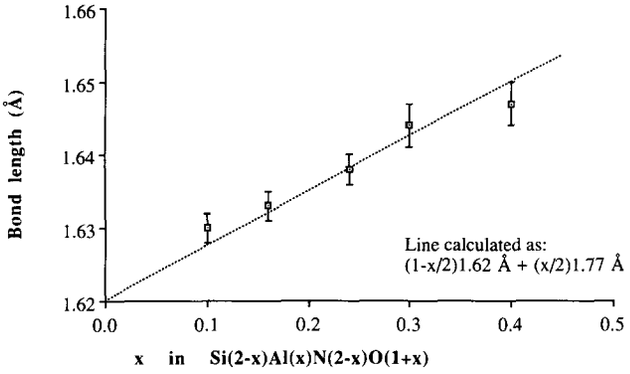

Fig. 2. Bond lengths (Si,Al)–O2 versus composition (in *x*) as calculated from the powder mixtures.

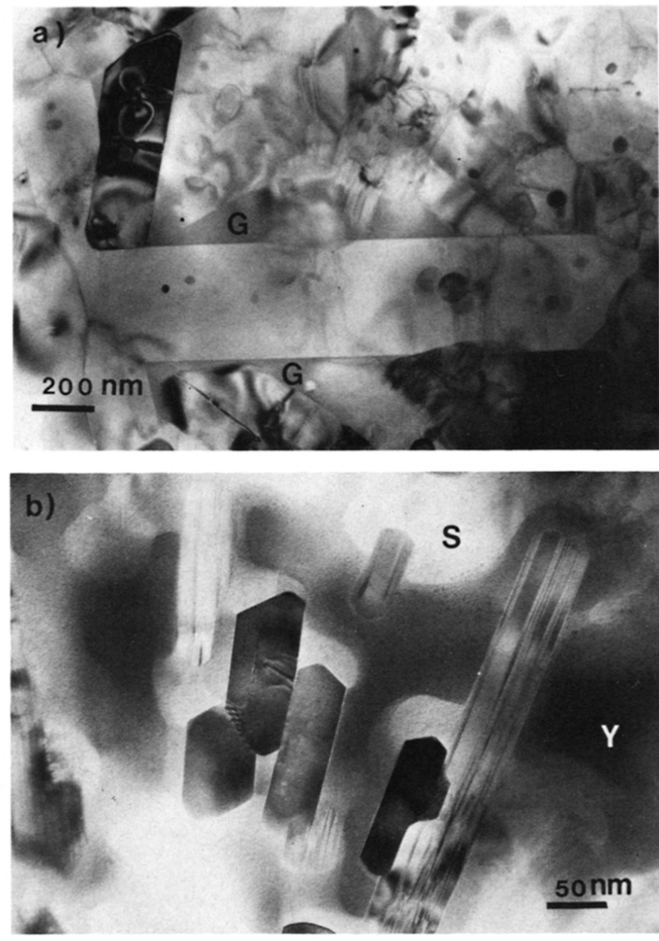

Fig. 3. TEM bright field images showing the general microstructure of (a) sample 11L where a large grain size distribution (0·1–5 μm) and small glass volume (G) are observed and (b) sample 13 where submicron size crystals are seen to be surrounded by a significant volume of glassy phase. The glass is phase separated into Y-rich (Y) and Si-rich (S) region.

composition expected from the powders used for syntheses. The theoretical bond length calculated from the expression $(1 - x/2)1{\cdot}62\,\text{Å} + (x/2)1{\cdot}77\,\text{Å}$, which is derived from data on related layered silicates[33] is indicated as a dotted line. In Table 5, occupancies estimated from the compositions of the starting powder mixtures are compared to those calculated in the Rietveld refinements (Table 4) and TEM/EDX microprobe analysis data for samples 11L and 13.

The microstructures of samples 11L and 13 are shown in Fig. 3(a) and (b), respectively. A general feature of the two samples is the glassy phase present, but there is considerably more glass present in sample 13, where a pronounced separation of the amorphous material into two glassy phases is observed (Fig. 3(b)). EDX analysis showed that although both regions contained Y, Si and Al, the glass with the dark contrast in Fig. 4 was richer in Y

Table 5. Expected compositions, calculated from powder mixtures, compared to Rietveld refinements and EDX analysis (calculated as *x*)

Sample	*Starting composition*	*Rietveld refinements*	*EDX*
2	0·10	0·17(6)	
3	0·16	0·20(6)	
4	0·24	0·36(6)	
10H	0·30	0·40(8) (Polaris) 0·30(8) (R2)	
11H	0·40	0·56(8)	
11L	0·40		0·19(6)
13	0·12		0·04(2)

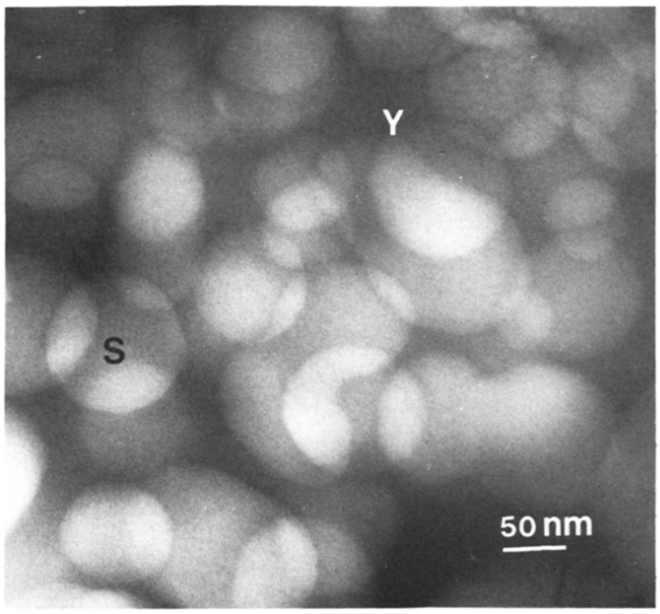

Fig. 4. A pocket of glass in sample 13 showing a typical metastable separation morphology. Spheroids of a light contrast glass (S) are contained in a continuous dark contrast glass (Y); TEM bright field.

Table 6. EDX analysis of O′-sialon crystals of samples 11L and 13 (wt% excluding N and O)

Sample		*Si*	*Al*	*Y*
11L		89(4)	9(3)	2(1)
13	O′Sialon crystals	98(1)	2(1)	
	Y-Rich glass	48(1)	14(1)	38(1)
	Si-Rich glass	80(3)	15(3)	15(3)

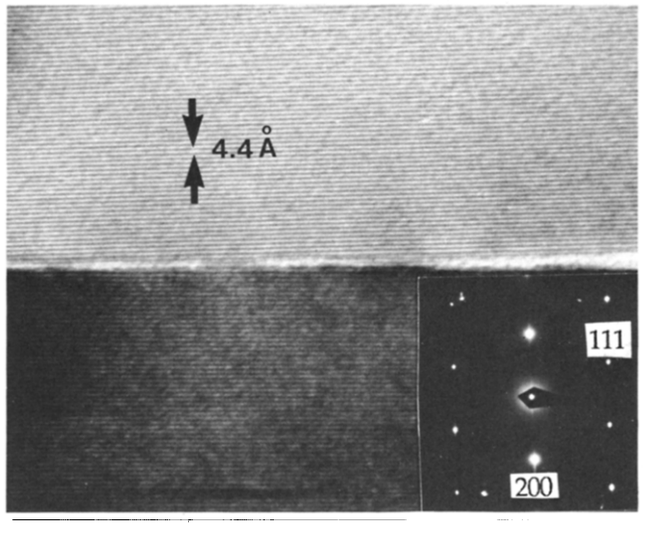

Fig. 5. Lattice fringe image and corresponding electron diffraction pattern of an O′-sialon crystal in sample 13 showing the preferred growth direction (*b*–*c* plane) of crystals grown from a liquid. The lattice fringes correspond to the (200) planes in the crystal (spacing 4·4 Å).

than the lighter contrast glass. The O′-sialon crystals were observed to grow from the more silicon-rich phase, forming plate-like crystals with a thickness of about 40 nm. The compositions of these crystals and of the two glasses, as well as those of sample 11L are given in Table 6. Electron diffraction pattern analysis and lattice fringe imaging showed that the preferred growth directions of the flat O′-sialon crystals are in the *b*–*c* plane of the unit cell (Fig. 5), in contrast to the single crystals prepared by gas-phase reaction, which grew along the *a*-axis.[32]

4 Discussion

4.1 Phase compositions

During sintering of the samples prepared from crystalline powders (samples 1–12L) *β′*-sialon is formed along with the major O′-sialon phase. It might be suggested that the presence of *β′*-sialon in all samples except 13 is due to oxygen deficiency which may have resulted from evaporation during sintering.[13] However, the high amount of oxides in all samples makes it more plausible that the formation of *β′*-sialon is due to kinetic effects, which would not be as strong in sample 13 where nitrogen and oxygen are more evenly distributed. The *α*-Si_3N_4 component observed in samples 1–12L is believed to be unreacted starting Si_3N_4. In sample 13, no crystalline secondary phases are observed. On post-sintering heat treatment of this sample, $Y_2Si_2O_7$ and SiO_2 were found,[25] although no additions of silica were made to this sample. The amorphous silicon oxynitride made from ammonia and silica, from which this sample was prepared, has been shown to be easily oxidised[34,35] and, despite the precautions taken, some nitrogen seems to have been lost. The composition of the remaining glass in sample 13 showed phase separation into two interwoven glasses, the compositions of which reflect the complicated equilibria at sintering and annealing temperatures in the system. Also in sample 11L glass separation had occurred, but there is more crystalline material in this case.

4.2 The composition of the O′-sialon crystals

Due to incomplete transformation to O′-sialon and losses by decomposition during sintering (typically less than 5 wt%) it is not expected that the compositions of the sintering materials can be derived directly from the starting composition. The increase in aluminium content is known to be reflected in an increased unit cell volume,[9] and this is also shown in Fig. 1 for the samples in this

investigation. For yttrium-free samples saturation is reached at $x \approx 0{\cdot}2$, in agreement with earlier work.[7] However, a continued growth of the unit cell volume with an increasing amount of aluminium in the starting mixtures at least up to $x = 0{\cdot}4$ is observed for the samples sintered with additions of yttria. The samples of set B sintered at 1928 K indicate a lower saturation limit than those exposed to the higher temperature, 1973 K, and have smaller unit cells for a given starting Al/Si ratio than both the samples of set A, which were sintered at 2093 K, and the samples of set B exposed to the higher temperature. There thus seems to be a temperature effect which is suggested, by the lattice parameters of samples 11L and 11H, and EDX analysis of sample 11L, to be an equilibrium effect (solubility of Al and O directly proportional to the temperature for the yttrium-containing samples). However, it is also possible that this is due to incomplete solution of aluminium and oxygen in the O′-sialons at the lower temperature.

Because of the presence of yttrium in the samples and the glassy phase remaining after sintering it is difficult to assign only on the basis of starting composition the observed differences in unit cell dimensions for the yttrium-containing samples to an increase in aluminium content of the O′-sialon crystals. The observed change in bond length (Si/Al)–O2 of samples 2, 3, 4, 10H and 11H (Fig. 2) is consistent with an increased aluminium content in the structure and provides an additional probe for the obtained composition. The agreement with the theoretical expression derived from cumulative data on layered silicates[33] is indeed good, and reflects the replacement of silicon by aluminium in the O′-sialon. Thus, x-values as high as 0·4 are supported.

The refinements of occupancy factors by the Rietveld technique on the data from ISIS also show that the amount of aluminium continues to increase throughout the set of five samples for which data were collected in the sequence predicted by the compositions of the starting powder mixtures. Although the relative correlation of the data is good, the absolute values of the derived occupancies are in poor agreement both with the calculated bond lengths and the starting compositions. This is a consequence of the fact that occupancy factors as well as the temperature factors from Rietveld refinements are known to be connected with uncertainties larger than the statistical error,[36,37] due to the models used, but also due to severe couplings between parameters. Bond lengths, calculated from refined atomic coordinates (which are not so strongly coupled to other parameters in Rietveld refinements and are therefore usually considered to be accurate within the calculated precision) from the R2 data are close to those derived from the ISIS data in this case. This shows that the refinements have been successful within the limits of the experiments and the refined models.

Investigation of elemental composition was carried out by EDX analysis of single grains of samples 11L and 13. For sample 11L the amount of aluminium found is lower than expected from the composition of the starting powder mixture, but the unit cell edge a determined for this sample is correspondingly shorter. As discussed, the smaller values of a for the yttrium-containing samples fired at the lower temperature cannot be compared to those of the samples fired at higher temperatures, because the equilibrium composition is not the same or has not been reached. If the refined lattice parameters of set A are taken as a 'standard', the agreement with the composition observed by EDX for sample 11L is good. The composition and lattice parameters of sample 13 are also compatible with this interpretation.

EDX analysis of sample 11L shows a small amount of yttrium to be present in the structure. The risk of picking up additional yttrium signal from the remaining glass surrounding the O′-sialon crystals is believed to be small, due to the care taken to select and analyse crystals lying at the edge of the specimen that were effectively free from glassy phase. The amount is not large enough to be responsible for the observed changes in lattice parameters or occupancy factors of the Si/Al site as determined by the Rietveld refinements based on neutron diffraction data. The refinements on the X-ray data on sample 10H failed to indicate any residual electron densities in addition to those found in the single-crystal refinement of Si_2N_2O,[32] which would be an indication of yttrium in the structure. The difficulties caused by the considerable contribution to the background from the amorphous material, forced exclusion of the low angle data from the refinement. However, the bond lengths calculated from the refined atomic coordinates are reasonable, and the low Bragg R-values derived in the calculations can therefore be considered meaningful.[36] The failure to observe electron densities in a Fourier difference plot of these refinements then shows that any presence of yttrium in the structure may be at the level determined by EDX, which is approximately one yttrium atom in every fifth unit cell, distributed over at least four possible sites in each cell.

From crystallographic considerations, inclusion of yttrium in the O′-sialon structure seems possible, e.g. approximately in the position (0, 0·71, 0·23),

where distances between yttrium and four oxygen atoms would be 2·43–2·75 Å. However, the low level of yttrium present is a strong indication that the inclusion of yttrium is not very favourable, although it might be essential to stabilise the aluminium-rich O′-sialons.

4.3 The importance of the composition of the melt

The increased solubility of aluminium in O′-sialon cannot, therefore, be explained solely by the presence of yttrium in the structure. The chemical nature of the liquid from which the O′-sialon is formed also may have an influence on the compositional range. However, comparison with other investigations where O′-sialons were prepared under conditions similar to those of this study does not give more relevant details. The work by Lewis *et al.*[13] showed negligible aluminium content for samples sintered at 1925 K with 6% Al_2O_3 and 10% Y_2O_3, in good agreement with the results for sample 13 which was sintered under similar conditions. Samples with compositions balanced to give $Y_2Si_2O_7$ as the secondary phase fired at 1975 K in a study by Trigg & Jack[15] showed a range of solubility ending at $x = 0{\cdot}15$. For yttrium-free samples synthesised by the reaction of Si_2N_2O and Al_2O_3 powders at 1825 K the maximum replacement is of about 15 mol%, i.e. $x = 0{\cdot}3$.[14]

It seems that the choice of starting mixtures to achieve a desired composition of the O′-phase is a delicate one. The scatter in the results obtained by different research groups may well be due to a variety of factors, such as incomplete mixing, impurities in starting powders and different heating schemes. The composition of the liquid will probably affect the equilibrium under which the O′-sialons are formed and retain aluminium outside the O′-sialons, or force it into solid solution, so that the total energy of the system is minimised. This can be expressed in terms of changes in the chemical potentials of the constituents of the liquid from which the O′-sialon formed, which may be sensitive to the presence of, for example, yttrium.

It is also necessary to consider the difficulties in reaching equilibrium for the different conditions used. This is seen from the differences observed for samples of identical compositions treated under slightly different time–temperature schemes (set B). It is indeed expected that equilibrium is more easily reached if the mobility of the components in the system is high. Mobility is favoured by high temperatures, but also the use of yttria as sintering aid is expected to lower the viscosity and favour saturation of O′-sialon with respect to aluminium. This is a possible explanation for the higher maximum aluminium contents found for samples of set B exposed to 1973 K than those for samples of set A.

4.4 The crystal morphology and growth

The role of reconstructive formation of O′-sialons and Si_2N_2O appears to manifest itself by the differences in preferred growth directions as observed for crystals formed from a liquid containing SiN_4 units and for those formed from a gas-phase containing SiO(g), respectively. In addition, stacking faults observed for O′-sialons precipitated from a melt are parallel to the *b*–*c* plane, while faults in the crystals formed from gas-phase reactions were along the *a*-axis. The observations for the sintered samples agree with those found by Lewis *et al.*,[13] who suggest the low solid–liquid surface energy of the (100) planes is responsible for these effects. The differences between crystals formed from a liquid and those prepared from gas-phase reactions also provide a reasonable explanation for the unexpectedly high value for unit cell edge *a* for the pure Si_2N_2O sample included in Table 3.

5 Conclusions

(1) The observed compositional range for the O′-sialons seems to depend considerably on the conditions under which they are prepared, e.g. the additives used and the temperature and the character of the sintering liquid.

(2) For the O′-sialons prepared by pressureless sintering at 2093 K, with Al_2O_3 only, the maximum aluminium content observed corresponds to $x \approx 0{\cdot}2$ in the general formula.

(3) For the O′-sialons prepared by pressureless sintering at 1973 K with additions of Al_2O_3 and 5 wt% Y_2O_3, the maximum *x*-value was $> 0{\cdot}4$.

(4) Some yttrium may enter the O′-sialon structure.

(5) The kinetics and the chemical potentials of the species in the liquid from which O′-sialon crystals precipitate are believed to be important factors affecting the solubility range.

Acknowledgements

The authors wish to thank Prof. R. Tellgren, Dr S. Hull, Mr H. Rundlöf and Mr P. Önnerud for their contributions in making the acquisition of high-

quality diffraction data possible. Travelling grants from the Swedish Natural Science Research Council are gratefully acknowledged.

References

1. Jack, K. H., The significance of structure and phase equilibria in the development of silicon nitride and sialon ceramics. *Sci. Ceram.*, **11** (1981) 125–42.
2. Ekström, T., Käll, P. O., Nygren, M. & Olsson, P. O., Dense single-phase β-sialon ceramics by glass-encapsulated hot isostatic pressing. *J. Mater. Sci.*, **24** (1989) 1853–61.
3. Lumby, R. J., North, B. & Taylor, A. J., Chemistry and creep of sialons. *Spec. Ceram.*, **6** (1974) 283–99.
4. Land, P. L., Wimmer, J. M., Burns, R. W. & Choudhury, N. S., Compounds and properties of the system Si–Al–O–N. *J. Am. Ceram. Soc.*, **61** (1978) 56–60.
5. Takase, A., Umebayashi, S. & Kishi, K., Infrared spectroscopic study of β-sialons in the system Si_3N_4–SiO_2–AlN. *J. Mater. Sci. Lett.*, **1** (1982) 529–32.
6. Takase, A. & Tani, E., Raman spectroscopic study of β-sialons in the system Si_3N_4–SiO_2–AlN. *J. Mater. Sci. Lett.*, **3** (1984) 1058–60.
7. Trigg, M. B. & Jack, K. H., Solubility of aluminium in silicon oxynitride. *J. Mater. Sci. Lett.*, **6** (1987) 407–8.
8. Gauckler, L. J., Lukas, H. L. & Petzow, G., Contribution to the phase diagram Si_3N_4–AlN–Al_2O_3–SiO_2. *J. Am. Ceram. Soc.*, **58** (1975) 346–7.
9. Jack, K. H., Sialons and related nitrogen ceramics. *J. Mater. Sci.*, **11** (1976) 1135–58.
10. Naik, I. K., Gauckler, L. J. & Tien, T. Y., Solid–liquid equilibria in the systems Si_3N_4–AlN–SiO_2–Al_2O_3. *J. Am. Ceram. Soc.*, **61** (1978) 332–5.
11. Sekercioglu, I. & Wills, R. R., Effect of Si_3N_4 powder reactivity on the preparation of the Si_2N_2O–Al_2O_3 silicon aluminium oxynitride solid solution. *J. Am. Ceram. Soc.*, **62** (1979) 590–3.
12. Wills, R. R., Sekercioglu, I. & Niesz, D. E., The interaction of molten silicon with silicon aluminium oxynitrides. *J. Am. Ceram. Soc.*, **63** (1980) 401–3.
13. Lewis, M. H., Reed, C. J. & Butler, N. D., Pressureless-sintered ceramics based on the compound Si_2N_2O. *Mater. Sci. Eng.*, **71** (1985) 87–94.
14. Cao, G. Z., Huang, Z. K., Fu, X. R. & Yan, D. S., Phase equilibrium studies in Si_2N_2O-containing systems: I. Phase relations in the Si_2N_2O–Al_2O_3–Y_2O_3 system. *Int. J. High Technol. Ceram.*, **1** (1985) 119–27.
15. Trigg, M. B. & Jack, K. H., Silicon oxynitride and O'-sialon ceramics. In *Proceedings of the First International Symposium on Ceramic Components for Engine*, ed. S. Somiya, E. Kanai & K. Ando. KTK Scientific Publishers, Tokyo, 1984, pp. 199–207.
16. Thompson, D. P., Phase relationships in Y–Si–Al–O–N ceramics. In *Tailoring Multiple and Composite Ceramics*, ed. R. E. Tressler, G. L. Messing, C. G. Pantano & R. E. Newnham. Plenum Publishing Co., 1986, pp. 79–91.
17. Slasor, S. & Thompson, D. P., Preparation and characterization of yttrium α'-sialons. In *Proceedings of the International Conference on Non-oxide Technical and Engineering Ceramics*, ed. S. Hampshire. Elsevier Applied Science, London, 1986, 223–30.
18. Thompson, D. P., Sun, W.-Y. & Walls, P. A., O'–β'- and α'–β'-sialon ceramics. In *Proceedings of the Second Initial Symposium on Ceramic Materials and Components for Engine*, ed. W. Bunk & H. Hausner. Deutsche Keramische Gesellschaft, Bad Honnef, 1986, pp. 643–50.
19. Huang, Z.-K., Griel, P. & Petzow, G., Formation of α-Si_3N_4 solid solutions in the system Si_3N_4–AlN–Y_2O_3. *J. Am. Ceram. Soc., Comm.*, **66** (1983) C-96–C-97.
20. Ekström, T., Effect of composition, phase content and microstructure on the performance of yttrium Si–Al–O–N ceramics. *Mater. Sci. Eng. A*, **A109** (1989) 341–9.
21. Trigg, M. B. & Jack, K. H., The fabrication of O'-sialon ceramics by pressureless sintering. *J. Mater. Sci.*, **23** (1988) 481–7.
22. Sjöberg, J., Rundgren, K., Osten-Sacken, J., Pompe, R. & Larsson, B., Nitridation of silica with ammonia: Some important features. *Sci. Ceram.*, **14** (1988) 205–10.
23. Johansson, K. E., Palm, T. & Werner, P.-E., An automatic microdensitometer for X-ray powder diffractions photographs. *J. Phys. E: Sci. Instrum.*, **13** (1980) 1289–91.
24. Werner, P.-E., A Fortran program for least-squares refinement of crystal-structure cell dimension. *Ark. Kemi*, **31** (1969) 513–16.
25. O'Meara, C. & Sjöberg, J., The development of microstructure in pressureless sintered Si_2N_2O bodies. *Ceram. Trans.*, **7** (1990) 647–63.
26. Hull, S. & Mayers, J., User guide for the polaris powder diffractometer at ISIS. Rutherford-Appleton Lab., RAL, 1989, **89–118**.
27. Lindqvist, O., Sjöberg, J. Hull, S. & Pompe, R., Structural changes in O'-sialons, $Si_{2-x}Al_xN_{2-x}O_{1+x}$, $0{\cdot}04 < x \leq 0{\cdot}40$. *Acta Cryst.*, **B47** (1991) 672–8.
28. David, W. I. F., Akporiaye, D. E., Ibberson, R. M. & Wilsson, C. C., The high resolution powder diffractometer at ISIS—An introductory users guide. Rutherford-Appleton Lab. Rep., RAL, 1988, **88–103**.
29. Wiles, D. B. & Young, R. A., A new computer program for Rietveld analysis of X-ray powder diffraction patterns. *J. Appl. Crystallogr.*, **14** (1981) 149–51.
30. Hill, R. J. & Howard, C. J., A computer program for Rietveld analysis of fixed wavelength X-ray and neutron powder diffraction patterns. *Aust. A.E.C. Res. Establ. Rep.*, AAEC/M112, 1986.
31. Lundgren, J.-O., Crystallographic computer programs. Uppsala Univ. Dep. Chem. Tech. Rep., UUIC-B13-4-05, 1982.
32. Sjöberg, J. Helgesson, G. & Idrestedt, I., Refinements of the structure of Si_2N_2O. *Acta Cryst.*, **C47** (1991) 2438–41.
33. Smith, J. V. & Bailey, S. W., Second review of Al–O and Si–O tetrahedral distances. *Acta Cryst.*, **16** (1963) 801–11.
34. Fink, P., Marx, G. & Meyer, K., Adsorptionseigenschaften und Struktur von chemisch modifizierten Siliciumdioxid- und Silicatoberflächen; 1) Die Wechselwirkung von Wasser und Aceton mit NH_3-modifizierten Aerosiloberflächen. *Z. Chem.*, **13** (1973) 314–15.
35. Marchand, R., Contribution à l'étude de quelques composés azotés et oxyazotés du silicium. *Rev. Chim. Miner.*, **7** (1970) 87–119.
36. Cheetham, A. K. & Taylor, J. C., Profile analysis of powder neutron diffraction data: Its scope, limitations, and applications in solid state chemistry. *J. Solid State Chem.*, **21** (1977) 253–75.
37. Albinati, A. & Willis, B. T. M., The Rietveld method in neutron and X-ray powder diffraction. *J. Appl. Crystallogr.*, **15** (1982) 361–74.